Commun Nonlinear Sci Numer Simulat 34 (2016) 66–76

Contents lists available at ScienceDirect

Commun Nonlinear Sci Numer Simulat

journal homepage: www.elsevier.com/locate/cnsns

Rogue wave formation under the action of quasi-stationary pressure

A.A. Abrashkin*, O.E. Oshmarina

National Research University, Higher School of Economics, 25/12 Bolshaja Pecherskaya str., 603155 Nizhny Novgorod, Russia

ARTICLE INFO

Article history:
Received 9 June 2015
Revised 27 August 2015
Accepted 7 October 2015
Available online 23 October 2015

Keywords:
Rogue waves
Exact solution
Vorticity
Lagrangian variables

ABSTRACT

The process of rogue wave formation on deep water is considered. A wave of extreme amplitude is born against the background of uniform waves (Gerstner waves) under the action of external pressure on free surface. The pressure distribution has a form of a quasi-stationary "pit". The fluid motion is supposed to be a vortex one and is described by an exact solution of equations of 2D hydrodynamics for an ideal fluid in Lagrangian coordinates. Liquid particles are moving around circumferences of different radii in the absence of drift flow. Values of amplitude and wave steepness optimal for rogue wave formation are found numerically. The influence of vorticity distribution and pressure drop on parameters of the fluid is investigated.

1. Introduction

Rogue waves also referred to as freak waves are waves of large amplitude that arise on sea surface all of a sudden and disappear just as quickly. Their characteristic feature is amplitude criterion according to which the height of rogue waves is twice or more the average height of the surrounding waves [1–4]. Being first considered for ocean waves, the concept has shifted to other fields of physics, such as nonlinear optics [5–8], physics of plasma [9], superfluid helium [10], and Bose-condensate systems [11]. Currently, of great interest is the elucidation of possible mechanisms of rogue wave formation and scenarios of their arising in different physical conditions that ultimately determine parameters and properties of extreme waves.

Rogue wave formation is a nonlinear effect [12] that was studied in the weakly nonlinear approximation within the framework of the nonlinear Schrödinger equation [13–21] and the Dysthe equation [22]. It was found that anomalous amplitude waves may arise as a result of modulation instability of initial perturbations of a definite class (see the reviews [1,4,23]). Dyachenko and Zakharov suggested that focusing of oceanic waves creates only preconditions for rogue wave formation, which is a strongly nonlinear effect. By solving a full system of equations of hydrodynamics they demonstrated that a rogue wave may be formed from a weakly nonlinear Stokes wave [24].

All the theoretical studies mentioned above were carried out for potential wave motion and constant pressure on free liquid surface. These assumptions are justified in the absence of wind. However, rogue waves frequently originate, when the wind impact cannot be neglected. Firstly, the wind changes pressure on the fluid surface, and secondly the wave motion becomes a vortex one. The first factor was taken into consideration in the works [25–30], where the dynamics of weakly nonlinear, narrow bandwidth trains of potential surface waves in the field of variable external pressure defined by the linear theory of wind wave excitation was investigated. Following Miles [31], but within the framework of modulated wave trains, those authors assumed

* Correspondence to. : Apt. 258, 6 Rokossovsky str., 603162 Nizhny Novgorod, Russia, Tel.: +7 9202946361.
E-mail address: aabrashkin@hse.ru (A.A. Abrashkin).

http://dx.doi.org/10.1016/j.cnsns.2015.10.006
1007-5704/

the atmospheric pressure at the interface due to wind and the water wave slope to be in phase, which is the necessary condition of energy transport from wind to moving waves. The evolution of the wave train envelope in this case is described by the nonlinear Schrödinger equation with an additional term proportional to the amplitude and ensuring its growth. Consequently, in this case the formation of extreme amplitude waves is determined by both, the modulation instability mechanism [32] and wind.

Yan and Ma studied rogue wave formation within the framework of a full system of equations of hydrodynamics and proposed a phenomenological formula for air flow pressure distribution on free surface [33], where pressure is a linear combination of wave slope and free surface elevation. The authors of [33] also showed that vortex air motion may be neglected in calculations of a maximum-height wave, but they did not analyze the role of liquid vorticity in its formation.

A vortex model of freak wave formation against the background of uniform waves was proposed in the paper [34] based on exact analytical solution of equations of 2D hydrodynamics of an ideal incompressible fluid [35,36]. A unique feature of flows of this class is the dependence of liquid particle motion coordinates on two complex functions that may be arbitrary to a great extent. As a consequence, the model may be used for analysis of different representations of surface pressure as well as liquid vorticity, i.e., taking into account simultaneously both these factors of air flow impact on the surface wave.

A partial exact solution for which the pressure of the free surface varied out of phase with the wave profile was investigated in [34]. Phillips in his book [37], however, emphasized that the phase difference between fluctuations of surface pressure and wave profile in natural environment may be very diverse, and statistical sampling of wave observations does not give unambiguous preference to any value or range of values. In this sense, it should be noted that Yan and Ma restricted applicability of their empirical formula and did not pretend it to be universal.

In the present work we consider the situation with surface pressure distribution qualitatively different from that in [34] within the framework of the class of exact solutions [35,36]. This distribution has a negative pressure pit, so that the elevation of the wave profile is first in phase with the pressure and then in antiphase. In this fashion we simulate a qualitatively self-consistent behavior of wave profile and pressure on it typical for oceanic and laboratory conditions [33,37]. The form of the exact solution is chosen so that pressure should be time independent in Lagrangian variables. In Euler variables, pressure is a function of time but the pit does not change its shape qualitatively. Unlike the nonstationary model considered in [34], the presented model may be called quasi-stationary. The properties of liquid flows for this model are determined by a single complex function.

Modulation instability is regarded to be one of the most probable mechanisms of extreme wave formation. In this respect, it is interesting to note that the role of modulation instability may increase significantly in the crossing sea states, when there are two wave systems (see [16,18,21] and references therein). However, the mechanism of anomalous wave formation considered in our paper is essentially different. It is based on nonuniform pressure distribution over liquid surface. Thus, the pressure gradient plays the part of external force in our model.

A new scenario of rogue wave formation has been found by means of numerical simulations. In the work [34], an extreme wave starts to grow from the Gerstner wave maximum, whereas in the new model it is born in the trough. The initial stage of uniform wave instability is characterized by an increase inside the trough of two local maxima corresponding to the edges of the pressure pit. We have studied the evolution of the vorticity field in the course of rogue wave formation and the influence of pressure drop on its height. Relations for parameters of maximum amplitude wave have been derived. The nonstationary and quasi-stationary models have been compared.

2. Ptolemaic waves on deep water

The equations of 2D hydrodynamics for waves on the surface of an incompressible inviscid fluid in Lagrangian coordinates are written in the following form [38]:

$$\frac{D(X,Y)}{D(a,b)} = \frac{D(X_0,Y_0)}{D(a,b)}, \tag{1}$$

$$X_{tt}X_a + Y_{tt}Y_a = -\frac{1}{\rho}p_a - gY_a, \tag{2}$$

$$X_{tt}X_b + Y_{tt}Y_b = -\frac{1}{\rho}p_b - gY_b, \tag{3}$$

where X, Y are Cartesian coordinates and a, b are Lagrangian coordinates of fluid particles, t is time, ρ is fluid density, p is pressure, g is acceleration of gravity, the subscripts mean differentiation by the corresponding variable, and the subscript "zero" means the value at time $t = 0$.

Eq. (1) is a volume conservation equation and Eqs. (2) and (3) are flow equations. Using the cross differentiation it is possible to exclude the pressure and to obtain the condition of vorticity conservation along the trajectory [38]:

$$(X_{ta}X_b + Y_{ta}Y_b - X_{tb}X_a - Y_{tb}Y_a)_t = 0. \tag{4}$$

Abrashkin and Yakubovich proposed to introduce complex Cartesian coordinates $W = X + iY$ ($\bar{W} = X - iY$) and complex Lagrangian coordinates $\chi = a + ib$ ($\bar{\chi} = a - ib$). Then Eqs. (1) and (4) are equivalent to the conditions of conservation of two

Jacobians [35,36]:

$$\frac{D(W,\bar{W})}{D(\chi,\bar{\chi})} = \frac{D(W_0,\bar{W}_0)}{D(\chi,\bar{\chi})} = D_0(\chi,\bar{\chi}),$$
$$\frac{D(W_t,\bar{W})}{D(\chi,\bar{\chi})} = \frac{D(W_{t0},\bar{W}_0)}{D(\chi,\bar{\chi})} = \frac{i}{2}D_0\Omega(\chi,\bar{\chi}). \tag{5}$$

Here Ω is vorticity, and the function D_0 defines the dependence of the initial position of fluid particles W_0 on Lagrangian variables. This function must not change the sign in the flow region. For simplicity, D_0 is assumed to be nonnegative.

(Eqs. 5) have an exact solution [35,36]:

$$W = G(\chi)e^{i\lambda t} + F(\bar{\chi})e^{i\mu t}, \tag{6}$$

where F, G are analytic functions, and λ, μ are real constants. The trajectories of the fluid particles are epicycloids (hypocycloids) as planet orbits in Ptolemaic system of the world, so the flows (6) were named Ptolemaic [35,36]. In the paper [36], Abrashkin and Yakubovich used the exact solution (6) for studying a single vortical domain in the surrounding potential flow. A whole class of Ptolemaic flows generalizing an elliptical Kirchhoff's vortex was described. Saffman has mentioned this paper in the monograph [39]. The monograph by Bennett [40] contains a detailed discussion of Ptolemaic flows. Guimbard and Leblanc studied the stability of Ptolemaic vortices [41].

The present paper, however, develops a different line of research. Let us consider the gravity waves on the surface of an infinitely deep fluid. Suppose that the motion of the fluid is described by expression (6). In Lagrangian coordinates the flow region corresponds to the domain $b = \mathrm{Im}\,\chi \le 0$. We study a particular case of Ptolemaic flows with $\lambda = 0,\ \mu = -\omega$:

$$W = G(\chi) + F(\bar{\chi})e^{-i\omega t}, \tag{7}$$

when fluid particles move in circles. The fluid is motionless at the bottom, so $|F| \to 0$ as $b \to -\infty$. The function G should be bijective, so $G' \neq 0$ in the flow region. One more requirement to the choice of the functions F, G is nonnegativity of the value of D_0:

$$D_0 = |G'|^2 - |F'|^2 \ge 0. \tag{8}$$

The vorticity of such a Ptolemaic wave is found from system (5) and is written as

$$\Omega = \frac{2\omega|F'|^2)}{|G'|^2 - |F'|^2}. \tag{9}$$

The pressure p is calculated from Eqs. (2) and (3) and is written in the form

$$\frac{p - p_0}{\rho} = -g\,\mathrm{Im}\left(G + Fe^{-i\omega t}\right) + \frac{1}{2}\omega^2|F|^2 + \mathrm{Re}\left(e^{i\omega t}\int \omega^2 G'\bar{F}d\chi\right) \tag{10}$$

where p_0 is a constant. The first term in expression (10) represents the well-known effect of "inverted barometer" [42]. In a general case, the pressure p oscillates periodically.

The Gerstner wave [38] belongs to the family of Ptolemaic flows. It is defined by the following expression:

$$W = \chi + iA\exp i(k\bar{\chi} - \omega t), \tag{11}$$

where A is amplitude, k is wave number, and ω is wave frequency. A dispersion equation for Gerstner waves has the form like for linear potential waves on deep water, i.e., $\omega^2 = gk$.

In the paper [34], a Ptolemaic flow of the form,

$$W = \chi - \frac{i\beta_*}{(\chi - i\alpha_*)^2} + \left[\frac{i\beta_*}{(\bar{\chi} + i\alpha_*)^2} + iA\,\exp(ik\bar{\chi})\right]\exp(-i\omega t), \tag{12}$$

where α_*, β_* are positive constants, was studied. The superposition principle holds true for Ptolemaic flows. If the function F is a sum of functions, the resulting profile qualitatively corresponds to the superposition of the profiles defined by these functions. When $\beta_* = 0$, expression (12) describes a Gerstner wave. The terms in F, G have one pole of order 2, which corresponds to $b = \alpha_* > 0$, so it is outside the fluid region. The term with the pole in the function F describes a periodically appearing peak. The term with the pole in the function G compensates the peak of the wave profile at the initial moment of time. So, expression (12) corresponds to the breather standing out in the field of the Gerstner wave. If the breather amplitude exceeds the amplitude A of the Gerstner wave more than twice, then according to the adopted criterion it may be called a rogue wave.

Such breather solutions also exist for other, more complicated presentations of functions G and F in expression (12). The function G defines the mean level of the free surface, and F specifies the radius and phase of liquid particle rotation around the circumference. Depending on their choice, the initial breather form and dynamics, as well as pressure distribution over free surface will change. Consequently, we can say that the breather solutions of the considered type exist for a wide class of distributed pressures.

For solving (12) we introduced qualitative changes to the form of pressure distribution on free surface during the oscillation period. At the initial moment of time, we observed a pressure pit relative to the constant (atmospheric) level p_a. The order of

magnitude of the pit was equal to α_*. Then it started to narrow, while its depth remained almost constant. Two elevations above the p_a level were formed on the left and right of the absolute pressure minimum. Half a period later, they reached their maximum (smaller than the pit depth). The rogue wave amplitude was maximal at this moment of time. It was decreasing gradually during the next half-period, and the pressure distribution recovered the form it had at the initial moment of time. During the oscillation period, the pressure on free surface changed significantly, determining the gravity wave dynamics.

In the present paper we consider a qualitatively different situation. Pressure above the region of rogue wave formation is always lower than the atmospheric level. The functions G and F are chosen so that pressure (10) should be time independent, i.e., it should be stationary in Lagrangian coordinates (it is nonstationary in Euler coordinates). The edges of the pressure pit shift with time, but its shape does not undergo qualitative changes. Rogue wave formation now occurs against the background of a quasi-stationary negative pressure drop. It is this drop that predetermines surface elevation, but now we can analyze kinematic features of rogue wave formation more explicitly and compare them with the known mechanisms inherent to extreme waves with constant pressure at a free boundary.

3. Solution for stationary pressure

We will address surface waves for which pressure (10) does not depend on time. This means that the functions F and G meet the following condition:

$$\mathrm{Im}\left[\left(g\bar{F} + i\omega^2 \int G'\bar{F}\,d\chi\right)\exp(i\omega t)\right] = 0.$$

It is fulfilled if the expression before the exponential factor is identical to zero. Differentiation of the equality

$$g\bar{F} + i\omega^2 \int G'\bar{F}\,d\chi = 0$$

with respect to χ yields

$$G' = \frac{ig}{\omega^2}\frac{\bar{F}'}{\bar{F}}. \tag{13}$$

By integrating this equation we find that the functions G and $\bar{F}$ are related by

$$G = \frac{ig}{\omega^2}\ln(\bar{F}/\alpha), \tag{14}$$

where α is a real constant of dimensional length (the value under the ln sign is dimensionless). Here, F is an arbitrary analytic function that has no singularities in the flow region $\mathrm{Im}\,\chi \le 0$. The function G is found by the know form of F from expression (14). The constant α in this expression specifies the horizontal scale of F variation. An additional requirement to choosing functions G and F is the condition of a nonnegative Jacobian (8). Making use of equality (13), the latter may be transformed to

$$\left|\frac{g}{\omega^2}\frac{F'}{F}\right| \ge \left|F'\right|. \tag{15}$$

The function F is represented in the form

$$F(\bar{\chi}) = iA\left(1 + \overline{P(\chi/\alpha)}\right)\exp(ik\bar{\chi}), \tag{16}$$

where A and k are the amplitude and wave number of the wave motion, respectively, and P is an analytical function. For $P = 0$, expressions (14) and (16) correspond to the Gerstner wave [38]. The pressure on the Gerstner wave profile is constant. Hereinafter, the function P will be chosen as a localized perturbation with horizontal scale α. At rather far distances from the perturbation ($|Re\,\chi| >> \alpha$), the solution of (7), (14), and (16) will transform to the Gerstner wave solution. Hence, the value of the wave number shall be chosen like in the Gerstner wave ($k = \omega^2/g$).

With the said above taken into consideration, inequality (15) is equivalent to fulfillment in the flow region of two conditions:

$$F'(\bar{\chi}) \ne 0, \quad |kF(\bar{\chi})| = \left|kA\left(1 + \overline{P(\chi/\alpha)}\right)\right| \le 1, \quad \mathrm{Im}\,\chi \le 0. \tag{17}$$

The first of them demands F (and, hence, P) to be a single-valued function, and the second limits the magnitude of wave perturbation amplitude. For the Gerstner wave ($P = 0$) it transforms to the inequality $kA \le 1$. The case of equality corresponds to a wave of limiting amplitude $A = k^{-1}$. The wave crest in this case coincides with the profile cusp (at this point the tangent to it is directed vertically).

Now we can write a partial form of the studied solution to (7) as

$$W = \chi + \frac{i}{k}\ln(1 + P(\chi/\alpha)) + iA\left(1 + \overline{P(\chi/\alpha)}\right)\exp i(k\bar{\chi} - \omega t) \tag{18}$$

This expression specifies a family of exact solutions dependent on one function P only. It must be analytical and bounded on the real axis, must meet conditions (17), and must not take on the value -1 in the flow region (to restrict the logarithmic term in (18)).

From the physical viewpoint, the first two terms in expression (18) determine an average level of fluid relative to which the liquid particles oscillate. The function $A(1+\overline{P(\chi/\alpha)})$ has the sense of a Gerstner wave train envelope. The case $\alpha >> \lambda = 2\pi/k$ corresponds to the wave train with slowly varying amplitude. Such wave motions are actively investigated within the framework of the nonlinear Schrödinger equation for the amplitude of wave train envelope under the condition of a potential flow and constant pressure on free surface. We, however, will be interested in the case of a strongly nonlinear wave train, when $\alpha << \lambda$. It corresponds to a breather evolving against the background of uniform Gerstner waves.

The pressure on free surface for the flow (18) is defined by

$$\frac{p-p_0}{\rho g} = \frac{k}{2}|F|^2 - \frac{1}{k}\ln|F/\alpha|, \quad \mathrm{Im}\chi = 0, \tag{19}$$

where F is given by equality (16). The value of the constant p_0 is taken to ensure the pressure on the free surface of a purely Gerstner wave (at $Re\,\chi \to \pm\infty$ and, hence, $P \to 0$) equal to the atmospheric pressure p_a. Then, expression (19) will be rewritten in the form

$$\frac{p-p_a}{\rho g} = \frac{k}{2}\left(|F|^2 - A^2\right) - \frac{1}{k}\ln|F/A|; \quad \mathrm{Im}\chi = 0. \tag{20}$$

We remind the reader that the pressure is time independent only in Lagrangian coordinates; whereas it is a function of time in Euler description.

The expression for the flow vorticity (18) will be written as

$$\Omega = \frac{2\omega k^2\left|A(1+\bar{P})\right|^2\exp(2kb)}{1-k^2\left|A\left(1+\bar{P}\right)\right|^2\exp(2kb)}. \tag{21}$$

In the absence of localized perturbation, when $P = 0$, the value of Ω is equal to the Gerstner wave vorticity [38].

4. Rogue wave against the background of Gerstner wave

Let us take the function P in the form

$$P(\chi/\alpha) = \frac{i\beta}{i\alpha - \chi}, \tag{22}$$

where β is a positive constant having dimension of length. This function has a pole at the point $\mathrm{Im}\chi = \alpha$, but by virtue of α positiveness this point is outside the flow region. Analogously, the point $\chi = (\beta+\alpha)i$, where P is equal to -1, corresponds to the region $\mathrm{Im}\chi > 0$ and is above the level of the fluid.

If $A = 0$, then the function F' equals zero. Let us assume $A > 0$, then the condition $F' = 0$ reduces to the equation

$$k(\bar{\chi} + i\alpha)^2 + ik\beta(\bar{\chi} + i\alpha) - \beta = 0, \tag{23}$$

the roots of which lie outside the flow region, i.e., in the half-plane $\mathrm{Im}\bar{\chi} < 0$. Assuming $\bar{\chi} = iw$ we rewrite Eq. (23) in the form

$$kw^2 + k(2\alpha+\beta)w + k\alpha(\alpha+\beta) + \beta = 0$$

As all the coefficients of this quadratic equation are positive, then according to the Rouse-Gurvitz criterion its roots must meet the condition $Re\,w = \mathrm{Im}\bar{\chi} < 0$. Consequently, for positive values of k, A, α, β, the function F' vanishes to zero only at the points corresponding to the inequality $\mathrm{Im}\,\chi > 0$.

The function $1+P$ is analytic, hence, it achieves its maximum value at the boundary of the flow region, where $\mathrm{Im}\,\chi = 0$. The inequality $|1+P| \le 1+(\beta/\alpha)$ holds for the absolute value of this function. With allowance for this inequality, (17) will be written in the following form:

$$kA\left[1+(\beta/\alpha)\right] \le 1. \tag{24}$$

The quantity β/α has an upper limit equal to $(1/kA)-1$. If the Gerstner wave steepness kA is close to zero, then β/α may have a very large value.

Fig. 1 shows the breather evolution and the pressure distribution on the free surface at different moments of time for the following values of parameters:

$$A = 2.5\,\mathrm{m}, \quad \alpha = 1\,\mathrm{m}, \quad \lambda = 30\,\mathrm{m}, \quad k = 0.21\,\mathrm{m}^{-1}, \quad \omega = \sqrt{gk} = 1\,\mathrm{c}^{-1}, \quad \beta = 0.9\,\mathrm{m}.$$

The minimum pressure is 100 mm Hg lower than the atmospheric pressure. The initial moment of time is $t_1 = \pi/\omega$.

Rogue wave formation starts in the Gerstner wave trough. A specific feature of this process is shown on a magnified scale in the inset on the left of the figure. First, two local maxima start to grow in the trough in the regions corresponding to the edges of the pressure pit. From this follows the conclusion that the pressure gradient force plays a decisive role at the initial stage of wave evolution. Later, at $t_2 = 5\pi/4\omega$, only the left maximum (for which $X < 0$) remains, with the geometrical center being shifted to the right, closer to the coordinate origin. At $t_3 = 3\pi/2\omega$, its height already exceeds the Gerstner wave amplitude; the elevation over the "amplitude level" has a nonsymmetric shape. At the next moment of time $t_4 = 7\pi/4\omega$, the amplitude

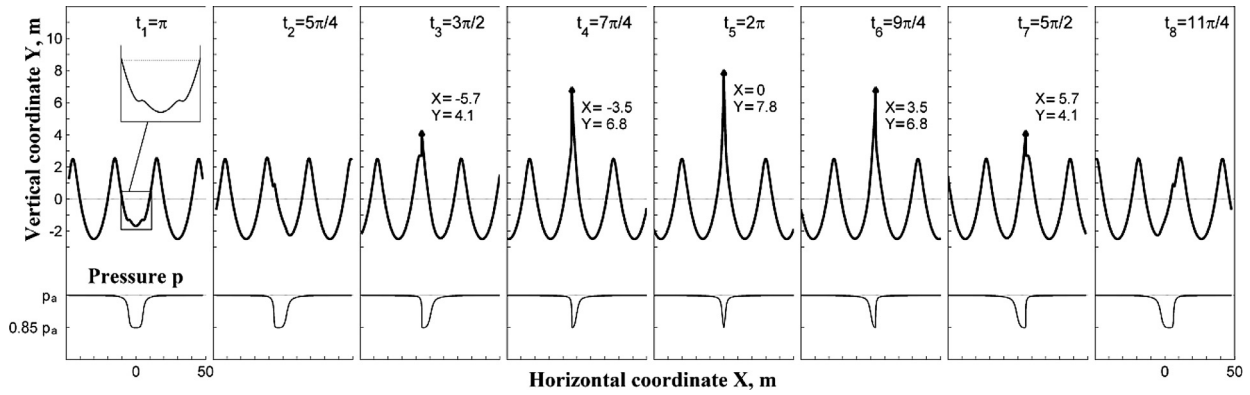

Fig. 1. Dynamics of free surface profile (upper curves) and pressure on free surface (lower curves) over one wave period. Numerical values for horizontal X and vertical Y coordinates are given for the wave crest.

of the peak grows and it becomes more symmetric. Finally, at $t_5 = 2\pi/\omega$ the wave height reaches its maximum and its profile becomes symmetric to the vertical $X = 0$. During the next half-period, the height of the peak decreases monotonically and its center shifts to the region of more and more positive X. The wave profile evolves analogously to the previous half-period: the pictures at $t_6 = 9\pi/4\omega$ and $t_4, t_7 = 5\pi/2\omega$ and $t_3, t_8 = 11\pi/4\omega$ and t_2 are mirror symmetric and transform one into another with the substitution $X \to -X$.

In the nonstationary model [34], a rogue wave starts to grow from the Gerstner wave maximum in the form of a single peak. The scenario proposed here has two principal distinctions: the rogue wave starts to form in the region of the Gerstner wave minimum and has a pair of spaced apart local elevations at the initial stage.

At the bottom of Fig. 1, pressure is plotted as a function of horizontal coordinate X at the corresponding moments of time. It is seen in the figure that the pressure deforms with time. It narrows during half a period and then widens to its previous state. An important property of the pressure drop is its negative value. We call the model with such pressure behavior quasi-stationary so as to distinguish it from the situation typical for Ptolemaic waves on water when pressure deviation from the atmospheric level in Lagrangian variables is an alternating-sign nonstationary function of time. Unlike the nonstationary model [34], the quasi-stationary model explicitly demonstrates the mechanism of rogue wave formation: the pressure pit is compressed along the horizontal and the fluid is forced to maximum possible height.

This mechanism of extreme wave formation is not connected with modulation instability. A solution arising as a result of modulation instability may be called free, whereas our solution is referred to the class of forced ones.

We consider a periodic solution, when a rogue wave is formed during a short time and disappears rapidly too. In our model it is equivalent to the fact that the external surface pressure "pit" generating an anomalous wave is formed and exists at times of the order of the wave period. For high enough waves to be formed large pressure drops are needed. We chose for numerical calculations a pressure drop of 100 mm Hg. Such pressure deviations are rare events realized at strong wind only. Besides, our model implies that these events are short-lived.

5. Wave parameters

5.1. Amplitude criterion

The wave height h is the most evident quantitative estimate of the wave size. It is defined as the vertical distance between the wave crest and the deepest trough preceding or following the crest. Frequently, a simple definition of a rogue wave is employed, according to which it is a wave that exceeds at least twice the significant wave height: $AI = H_{max}/H_s > 2$, here H_{max} is the height of the rogue wave, and H_s is the significant wave height which is the average of the third of highest waves in a time series. The ratio of these heights is referred to as "abnormality index" and is denoted by AI. In our model the amplitude A and the freak wave height h are calculated relative to the still water level, so $H_{max} = h + A,\ H_s = 2A$ and the amplitude criterion for rogue waves takes on the form $AI = h/A > 3$.

The peak height h relative to the still water level can be estimated using Eqs. (18) and (22) at the moment of time $t_4 = 2\pi/\omega$ at the point $\chi = 0$. The peak height equals

$$h = \frac{1}{k}\ln(1+\beta) + A(1+\beta). \tag{25}$$

Hereinafter we will assume for simplicity $\alpha = 1$ m; consequently, β will be considered to be a dimensional quantity. For maximum possible value of β equal to $\beta_{max} = (1/kA) - 1$, the height of the maximum wave peak is

$$h = \frac{1 - \ln(kA)}{k}, \tag{26}$$

Table 1
Abnormality index as a function of Gerstner wave steepness.

kA	0.10	0.20	0.30	0.35	0.40	0.45	0.5	0.55
h/A	33	13	7.3	5.9	4.8	4	3.4	2.9

and the abnormality index is written in the form

$$AI = \frac{h}{A} = \frac{1 - \ln(kA)}{kA}.$$

It depends on the Gerstner wave steepness only and its magnitude decreases monotonically down to unity with steepness increasing up to $kA = 1$. The law of h/A variation as a function of kA is demonstrated in Table 1.

Based on this table and the amplitude criterion we can conclude that freak waves do not arise in this model, if $kA > 0.55$.

In the calculations presented in Fig. 1, the Gerstner wave steepness was taken to be $kA = 0.52$, and the abnormality index was $AI = 3.13$.

We chose the steepness parameter for the following reason: From Table 1 it is clear that the abnormality index is a conditional quantity to a certain extent. For small enough steepness, the value of AI may amount to several tens, whereas the rogue wave amplitude remains very small. Consequently, we chose for out numerical computations the value of steepness such that, on the one hand, the amplitude criterion should be still fulfilled ($AI = 3.13 > 3$), and on the other hand, maximum elevation of the rogue wave should be as high as possible $h = 7.8$ m, see (Fig. 1).

5.2. Vorticity

Expression (21) for wave vorticity taking into account (22) for the function P has the following form:

$$\Omega = 2\omega k^2 A^2 \frac{\left[(\beta + 1 - b)^2 + a^2\right]\exp(2kb)}{(1-b)^2 + a^2 - k^2A^2\left[(\beta + 1 - b)^2 + a^2\right]\exp(2kb)},$$

a, b, β in the polynomial terms are made dimensionless to $\alpha = 1$ m. There are two regions in the vorticity field. The first of them is formed by the particles the Lagrangian coordinates of which meet the inequality

$$|\chi - i| = \sqrt{(1-b)^2 + a^2} >> \beta. \tag{27}$$

The expression for vorticity for this region is written as

$$\Omega_G = \frac{2\omega k^2 A^2 \exp(2kb)}{1 - k^2A^2\exp(2kb)}.$$

It coincides with the Gerstner wave vorticity (that's where the subscript "G" comes from). The quantity Ω_G is a function of vertical Lagrangian coordinate b only and is constant on its isolines. For Gerstner waves, $b = const$ are periodic curves similar to the wave profile [38].

The second region of the vorticity field is formed by the particles for which the inequality (27) is not fulfilled. It is the area where a rogue wave is formed. Vorticity for the particles inside it depends on both Lagrangian coordinates. Vorticity isolines for the body of particles directly participating in the formation of the wave crest are shown in Fig. 2. The vortex lines in this flow region originate and terminate on free surface. Five moments of time from t_1 to t_5 are taken. At the initial moment of time t_1, the vortex lines are symmetric concave lines. In the next quarter of the period (from t_2 to t_3), their left edge steepens. Then (from t_3 to t_4), the right edge begins to steepen, so that at the moment of the highest wave elevation, the vortex lines become symmetric again. In the immediate vicinity of the wave crest, the vortex lines become convex. The light gray isolines correspond to the smaller vorticity, and the black ones to greater vorticity.

As seen from the expression (21), the vorticity is maximum at the maximum points of the absolute value of the function $1 + P$, i.e., at the point $a = 0$, $b = 0$. This point in Fig. 2 is denoted by m. It is in the center of the trough at the initial moment of time. Then, in the motion around the circumference (the property of Ptolemaic flows) it ascends higher and higher and at t_5 it coincides with the point of the maximum elevation of the rogue wave. Thus, in the considered model the wave attains maximum height when the particle with maximum vorticity becomes its crest.

5.3. Pressure drop

Another important parameter determining the properties of a rogue wave in this model is a characteristic magnitude of pressure drop (pressure pit depth). From Fig. 1 it is clear that the pressure distribution on free surface is minimum at the point $\chi = 0$. Making use of (20), we will find pressure deviation Δp from the level of atmospheric pressure

$$\frac{\Delta p}{\rho g} = \left.\frac{p - p_a}{\rho g}\right|_{\chi=0} = \frac{1}{2}kA^2(2\beta + \beta^2) - \frac{1}{k}\ln(1+\beta). \tag{28}$$

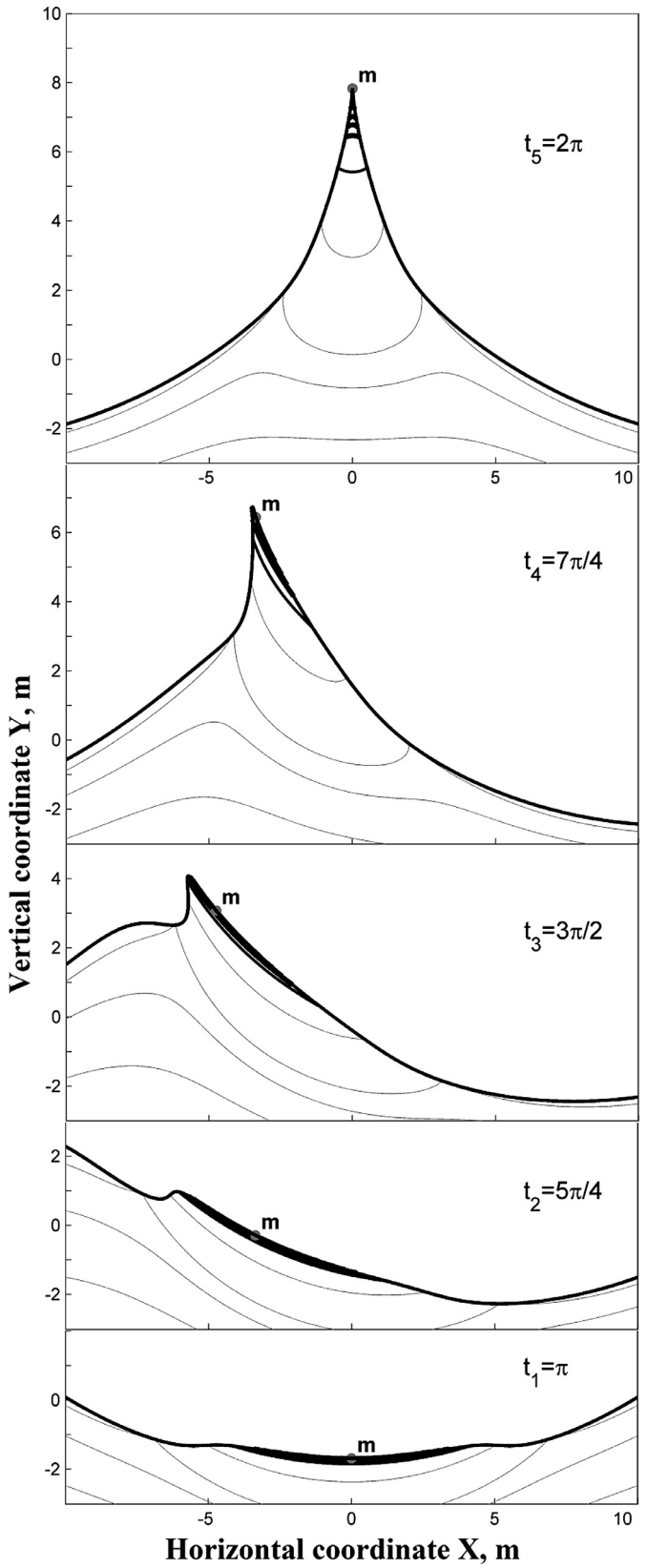

Fig. 2. Vorticity isolines in the region of the wave crest at different moments of time. Dark lines correspond to larger vorticity. Point *m* denotes maximum vorticity isoline.

We will show that $\Delta p$is always negative, if $\beta > 0$. Assume that the inverse is true and the inequality

$$k^2A^2(2\beta + \beta^2) \geq \ln(1+\beta)^2, \quad \beta \geq 0$$

is fulfilled. By substituting $z = (1+\beta)^2$ we can rewrite it as

$$k^2A^2(z-1) \geq \ln z, \quad z \geq 1. \tag{29}$$

At the point$z = 1$, the left- and right-hand sides of the inequality coincide and are equal to zero. The derivatives of the left- and right-hand sides are, respectively, $d_1 = k^2A^2$ and $d_2 = 1/z$, and are related to

$$\frac{d_1}{d_2} = k^2A^2z = k^2A^2(1+\beta)^2 \leq k^2A^2(1+\beta_{max})^2 = 1.$$

Here, the equality sign corresponds to β_{max} or to the maximum possible value of $z = 1/(kA)^2$. With increasing z the left side grows slower than the right one, hence, the inequality (29) has only one solution $z = 1$ or $\beta = 0$. But this means that our assumption is wrong and the pressure drop $\Delta p$is always negative.

For maximum possible value $\beta = \beta_{max}$ the relation (28) is rewritten in the form

$$\frac{\Delta p}{\rho g A} = \frac{3}{2kA} - \frac{1}{2}kA - \frac{h}{A}. \tag{30}$$

It relates four parameters of the model: characteristic pressure drop Δp, maximum peak height h, as well as amplitude A and wave number k of the Gerstner wave. From (30) it follows that the rogue wave will be the higher, the more the pressure drop is. Formula (30) may be a dynamic condition relating the parameters of the maximum rogue wave, whereas the equality (26) that does not contain pressure drop plays the role of kinematic condition.

5.4. The dependence of maximum rogue wave height on Gerstner wave parameters

The rogue wave height is determined by four parameters: Gerstner wave amplitude A, its wavelength λ (or wave number $k = 2\pi/\lambda$), magnitude of the vertical scale of perturbation above the Gerstner wave crests β (β/α, if $\alpha \neq 1$ m), and pressure drop Δp. The region of admissible values of β has the upper limit β_{max} determined by wave steepness. The magnitude of pressure drop is chosen from physical considerations. The numerical computations were done for $\Delta p = -100$ mm Hg. Such pressure drops occur, in particular, inside whirlwind and tornado. With a restriction on the choice of parameters β and Δp, we will study the dependence of maximum freak wave height h on Gerstner wave parameters.

The plots for $h(A)$ at a constant value of Gerstner wave steepness are presented in Fig. 3. Three typical values of steepness are chosen. Each plot consists of two sections. One of them is rectilinear and is specified by the formula (26). It corresponds to the case $\beta = \beta_{max}$, and the absolute value of the pressure drop does not exceed 100 mm Hg. The second section is curvilinear, it

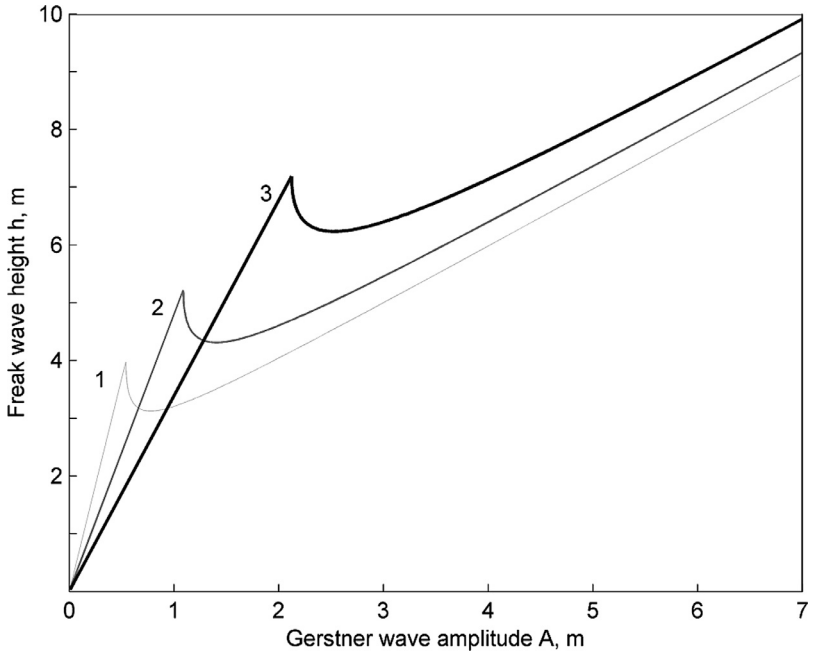

Fig. 3. Maximum possible rogue wave height versus background Gerstner wave amplitude at constant steepness and pressure drop not more than 100 mm Hg. Curves 1, 2, and 3 correspond to the values of steepness $kA = 0.3;\ 0.4;\ 0.5$, respectively.

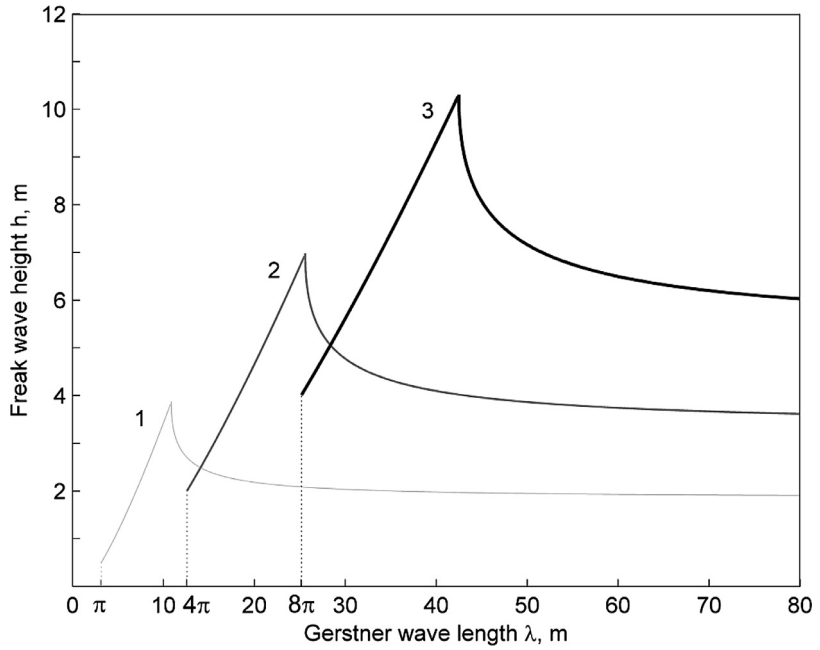

Fig. 4. Maximum possible rogue wave height versus background Gerstner wave length at constant amplitude and pressure drop not more than 100 mm Hg. Curves 1, 2, and 3 correspond to the values of amplitude $A = 0.5$ m; 2 m; 4 m, respectively.

refers to higher amplitude values and corresponds to the case when $\beta \le \beta_{max}$ and $|\Delta p| = 100$ mm Hg. This section of the $h(A)$ curve is specified parametrically by relations (25) and (28), where β is a parameter. A similar technique is also used for plotting rogue wave height versus Gerstner wavelength at a constant value of its amplitude.

The function $h(\lambda)$ is plotted in Fig. 4. Here, the linear sections correspond to the maximum values of β, and the curvilinear ones to the limit quantity of the pressure drop. As $kA \le 1$ for the Gerstner wave, the region of possible wavelengths is specified by the inequality $\lambda \ge 2\pi A$. For long waves, h slowly decreases with increasing wavelength and at $\lambda \to \infty \quad (\beta \to 0)$ tends to the Gerstner wave amplitude. The kinematic condition is decisive in the region of small amplitudes (Fig. 3) and wavelengths (Fig. 4), and the dynamic condition is essential in the region of large values. Fig. 4 demonstrates that for each fixed amplitude of Gerstner wave there exists a definite wavelength at which a freak wave achieves maximum height.

Fig. 3 demonstrates how the factor of restricted pressure drop affects rogue wave height. In the case of small-amplitude and small-steepness Gerstner waves, the rogue wave may possess a very large abnormality index AI, but its maximum height is relatively small. On the other hand, for large values of A, the rogue wave height reaches rather high values but no longer meets the amplitude criterion. The optimum steepness for high rogue waves to appear is $kA = 0.3 \div 0.6$. The nonstationary model described in [34] may be called a "weak steepness" model, whereas the quasi-stationary model may be referred to as a "middle steepness" model.

The exact solution (6) obtained in [35,36] determines self-consistently pressure on free surface. Its remarkable property is the dependence on two arbitrary functions of Lagrangian coordinates G and F. This means that, for the pressure changing harmonically in time, the form of its initial distribution on the surface may be chosen to be quite arbitrary (taking into consideration restrictions on the choice of these functions). In our paper we study the case when only one of these functions is free. The class of possible surface pressure distributions becomes narrower in this case but there appear more opportunities for detailed analytical investigation of the properties of rogue wave and relationship of its parameters.

All the computations presented in Sections 4 and 5 were performed for the function P that has a rather simple form and allows using analytical methods. At the same time, our analysis shows that analogous wave regimes of liquid motion are quite possible at other quasi-stationary surface pressure distributions (other representations of the function P) qualitatively similar to those considered in this paper. This enables us to conclude that the studied example represents a rather general situation, and rogue waves of this type may be observed in the real ocean.

It is important to note that the proposed model may be tested in a tank equipped with a wave generator and a wind tunnel.

6. Conclusion

A family of exact solutions for surface gravity vortex waves on deep water at stationary pressure distribution on free surface in Lagrangian coordinates was constructed within the framework of Ptolemaic flows. The wave profile and fluid motion depend on the analytic function of a rather arbitrary form. We investigated the process of rogue wave formation against the background of Gerstner waves for a particular form of the function corresponding to the surface pressure pit. The relations for calculating

maximum height of rogue wave by given uniform wave parameters at a given pressure drop were derived. It was shown that the presented quasi-stationary model differs from the nonstationary model studied earlier by the kinematic features of rogue wave formation.

Acknowledgments

The article was prepared within the framework of the Academic Fund Program at the National Research University Higher School of Economics (HSE) in 2015 (Grant no. 15-01-0044) and supported within the framework of a subsidy granted to the HSE by the Government of the Russian Federation for the implementation of the Global Competitiveness Program.

References

[1] Dysthe K, Krostad HE, Müller P. Oceanic rogue waves. Annu Rev Fluid Mech 2008;40:287–310.
[2] Osborne AR. Nonlinear ocean waves. Academic Press; 2009.
[3] Kharif C, Pelinovsky E, Slunyaev A. Rogue waves in the ocean. Berlin: Springer-Verlag; 2009.
[4] Slunyaev A, Didenkulova I, Pelinovsky E. Rogue waves. Contemp Phys 2011;52(6):571–90.
[5] Solli DR, Ropers C, Koonath P, Jalali B. Optical rogue waves. Nature 2007;450:1054–7.
[6] Onorato M, Proment D, Toffoli A. Triggering rogue waves in opposing currents. Phys Rev Lett 2011;107:184502 4p.
[7] Akhmediev N, Soto-Crespo JM, Ankiewicz A. How to excite a rogue wave? Phys Rev A 2009;80:043818 7p.
[8] Zhao LC, Liu C, Yang ZY. The rogue waves with quintic nonlinearity and nonlinear dispersion effects in nonlinear optical fibers. Commun Nonlinear Sci Numer Simul 2015;20(1):9–13.
[9] Moslem WM, Shukla PK, Eliasson B. Surface plasma rogue waves. Europhys Lett 2011;96(2):25002 4p.
[10] Efimov VB, Ganshin AN, Kol'makov GV, McClintock PVE, Mezhov-Deglin LP. Rogue waves in superfluid helium. Eur Phys J Spec Top 2010;185:181–93.
[11] Wen L, Li L, Li Z, Song S, Zhang X, Liu W. Matter rogue wave in Bose–Einstein condensates with attractive atomic interaction. Eur Phys J: D 2011;64(2–3):473–8.
[12] Ruban V, Kodama Y, Ruderman M, Dudley J, Grimshaw R, McClintock PVE, et al. Rogue waves – towards a unifying concept?: Discussions and debates. Eur Phys J Spec Top 2010;185(1).
[13] Peregrine DH. Water waves, nonlinear Schrödinger equations and their solutions. J Aust Math Soc Ser B 1983;25:16–43.
[14] Ankiewicz A, Kedziora D, Akhmediev N. Rogue wave triplet. Phys Lett A 2011;375(28):2782–5.
[15] Ankiewicz A, Devine N, Akhmediev N. Are rogue waves robust again perturbations? Phys Lett A 2009;373(43):3997–4000.
[16] Onorato M, Jsborne AR, Serio M. Modulational instability in crossing sea states: a possible mechanism for the formation of freak waves. Phys Rev Lett 2006;96:014503 5p.
[17] Dyachenko AI, Zakharov VE. On the formation of freak waves on the surface of deep water. JETP Lett 2008;88:307–11.
[18] Toffoli A, Bitner-Gregersen EM, Osborne AR, Serio M, Monbaliu J, Onorato M. Extreme waves in random crossing seas: laboratory experiments and numerical simulations. Geophys Res Lett 2011;38:L06605 5p.
[19] Chabchoub A, Hoffman NP, Akhmediev N. Rogue wave observation in a water wave tank. Phys Rev Lett 2011;106:204502 4p.
[20] Kedziora DJ, Ankiewicz A, Akhmediev N. Classifying the hierarchy of nonlinear-Schrödinger-equation rogue-wave solutions. Phys Rev E 2013;88(1):013207 12p.
[21] Ablowitz MJ, Horikis TP. Interacting nonlinear wave envelopes and rogue wave formation in deep water. Phys of Fluids 2015;27:012107 10p.
[22] Ablovitz MJ, Hammack J, Henderson D, Scholder SM. Modulated periodic Stokes waves in deep water. Phys Rev Lett 2000;84:887–90.
[23] Kharif C, Pelinovsky E. Physical mechanisms of the rogue wave phenomenon. Eur J Mech B Fluids 2003;22:603–34.
[24] Dyachenko AI, Zakharov VE. Modulation instability → freak wave. JETP Lett 2005;81(6):255–9.
[25] Leblanc S. Amplification of nonlinear surface waves by wind. Phys Fluids 2007;19(10):101705.
[26] Kharif C, Giovanangeli J-P, Touboul J, Grare L, Pelinovsky E. Influence of wind on extreme wave events: experimental and numerical approaches. J Fluid Mech 2008;594:209–47.
[27] Adcock TAA, Taylor PH. Energy input amplifies nonlinear dynamics of deep water wave groups. Int J Offsh Polar Eng 2011;21(1):8–12.
[28] Onorato M, Proment D. Approximate rogue wave solutions of the forced and damped nonlinear Schrödinger equation for water waves. Phys Lett A 2012;376(45):3057–9.
[29] Chabchoub A, Hoffman N, Branger H, Kharif C, Akhmediev N. Experiments on wind-perturbed rogue wave hydrodynamics using the Peregrine breather model. Phys Fluids 2013;25(10):101704 4p.
[30] Brunetti M, Marchiando N, Berti N, Kasparian J. Nonlinear fast growth of water waves under wind forcing. Phys Lett A 2014;378(14):1025–30.
[31] Miles JW. On the generation of surface waves by shear flows. J Fluid Mech 1957;3(2):185–204.
[32] Kharif C, Kraenkel RA, Manna MA, Thomas R. The modulational instability in deep water under the action of wind and dissipation. J Fluid Mech 2010;664:138–49.
[33] Yan S, Ma QW. Improved model for air pressure due to wind on 2D freak waves in finite depth. Eur J Mech B Fluids 2011;30(1):1–11.
[34] Abrashkin AA, Soloviev A. Vortical freak waves in water under external pressure action. Phys Rev Lett 2013;110:014501 4p.
[35] Abrashkin AA, Yakubovich EI. Vortex dynamics in a lagrangian description, Moscow: Fizmatlit; 2006. (in Russian).
[36] Abrashkin AA, Yakubovich EI. Planar rotational flows of an ideal fluid. Sov Phys Dokl 1984;29:370–4.
[37] Phillips OM. The dynamics of the upper ocean. Cambridge: Cambridge University Press; 1977.
[38] Lamb H. 6th ed. Hydrodynamics. Cambridge: Cambridge University Press; 1932.
[39] Saffman PG. Vortex dynamics. Cambridge: Cambridge University Press; 1992.
[40] Bennett A. Lagrangian fluid dynamics. Cambridge: Cambridge University Press; 2006.
[41] Guimbard D, Leblanc S. Local stability of the Abrashkin–Yakubovich family of vortices. J Fluid Mech 2006;567:91–110.
[42] Wunsch C, Stammer D. Atmospheric loading and the oceanic inverted barometer effect. Rev Geophys 1997;35(1):79–107.